IEICE TRANS. FUNDAMENTALS, VOL.E107–A, NO.8 AUGUST 2024

LETTER

Permanent Magnet Synchronous Motor Speed Control System Based on Fractional Order Integral Sliding Mode Control

Jun-Feng LIU[†], **Yuan FENG**[†], **Zeng-Hui LI**[†], *and* **Jing-Wei TANG**[††a)], ***Nonmembers***

SUMMARY To improve the control performance of the permanent magnet synchronous motor speed control system, the fractional order calculus theory is combined with the sliding mode control to design the fractional order integral sliding mode sliding mode surface (FOISM) to improve the robustness of the system. Secondly, considering the existence of chattering phenomenon in sliding mode control, a new second-order sliding mode reaching law (NSOSMRL) is designed to improve the control accuracy of the system. Finally, the effectiveness of the proposed strategy is demonstrated by simulation.

key words: *permanent magnet synchronous motors, fractional order calculus, second order sliding mode, chattering, robustness*

1. Introduction

With the development of control theory, computer technology, etc., the application of advanced, intelligent control to the control of permanent magnet synchronous motor (PMSM) has given PMSM new opportunities. Sliding mode control (SMC) is characterized by its simple structure, robustness to uncertainties such as system parameters and external disturbances, and fast response, which makes it a hot research topic when applied to the field of motor control [1]. However, its application is limited by the problem of inherent chattering.

In order to reduce chattering and improve its control performance, scholars have combined SMC with adaptive control [2], fuzzy control [3], neural network control [4] and so on to achieve better results, but its algorithm becomes complex, weakening the advantages of SMC algorithm is simple and fast response. For this reason, some scholars have proposed integral sliding mode control (ISMC) by introducing an integral term on the sliding mode surface to improve the robustness of the system while weakening the chattering [5]. However, it has a cumulative effect on the error, if the initial error is large or the reference signal changes will cause the integral saturation, which will lead to the system overshooting increases, the regulation time becomes longer, and deteriorate the dynamic performance of the system [6].

In sliding mode control, the discontinuity of the traditional reaching law is directly transferred to the control, and the frequent switching causes chattering, which affects the system control accuracy. For this reason, a new variable exponential reaching law according to the system state change is proposed in the literature [7] to suppress the sliding mode chattering. However, its parameters are too many and the tuning parameter is too cumbersome. Literature [8] applies a second-order sliding mode reaching law to induction motor speed loop control, which suppresses chattering by placing discontinuous switching functions with large gain values in the integration term. However, the control gain of this reaching law needs the disturbance term to be differentiable, and there is a specific boundary value, the precise value of this boundary in practical applications, it is difficult to determine, in order to get the stable control of the system, often selected as large as possible parameter, which results in bringing the system damage and violent chattering [9].

In order to solve this problem, this paper combines the fractional order calculus theory [10] with the integral sliding mode control to design a fractional order integral sliding mode surface, which improves the robustness and stability of the system under the premise of reducing the static error of the system. Secondly, a new second-order sliding mode reaching law is introduced to suppress the sliding mode chattering, which further improves the control accuracy of the system. Finally, the effectiveness of the proposed strategy is verified by simulation experiments.

2. Mathematical Model of PMSM

To facilitate the modeling, this paper adopts the surface-mounted PMSM (SPMSM) with equal stator inductance $L_d = L_q = L_s$, which is expressed as follows:

$$\begin{cases} \dfrac{di_d}{dt} = -\dfrac{R}{L_s} i_d + \omega_e i_q + \dfrac{u_d}{L_s} \\ \dfrac{di_q}{dt} = -\dfrac{R}{L_s} i_q - \omega_e i_d - \dfrac{\varphi_f}{L_s}\omega_e + \dfrac{u_q}{L_s} \end{cases} \tag{1}$$

Where i_d, i_q, u_d, u_q stands for the stator current as well as stator voltage inside the d-q coordinate system, separately, R is the stator resistance, ω_e represents the electrical motor angular speed; φ_f represents magnetic flux.

For SPMSM, using the vector control method with $i_d = 0$, the formulation of motion is listed below [11]:

$$\begin{cases} J\dfrac{d\omega_m}{dt} = T_e - T_L - B\omega_m \\ T_e = 1.5 p i_q \varphi_f \end{cases} \tag{2}$$

Manuscript received January 31, 2024.
Manuscript publicized March 4, 2024.
[†]Zhengzhou Railway Vocational & Technical College, Zhengzhou, 451460 China.
[††]Hunan College of Information, Changsha, 410200 China.
a) E-mail: tang2021048@163.com
DOI: 10.1587/transfun.2024EAL2012

Where T_L, T_e, ω_m, p, B and J are the load torque, the electromagnetic torque, mechanical angular speed, the quantity of pole pairs, damping coefficient as well as rotational inertia respectively.

3. Design of Speed Controller

3.1 Design of Sliding Mode Surface

First, define the state variable as:

$$\begin{cases} e = \hat{\omega} - \omega \\ \dot{e} = -\dfrac{\left(1.5pi_q\varphi_f - T_L - B\omega\right)}{J} \end{cases} \tag{3}$$

Where $\hat{\omega}$ is the given speed of the motor, ω is the actual speed of the motor, $\hat{\omega} = \frac{30}{\pi}\omega_{\mathrm{m}}$.

The integral sliding mode surface is [12]:

$$s = e + g\int edt \tag{4}$$

Where g is the constant. Due to the cumulative effect of the integral term on the deviation, the dynamic performance of the control system can be deteriorated when the initial error is large or when the integral saturation phenomenon tends to occur when there is a sudden change in the given signal. To solve this problem, the fractional order integral sliding mode surface is designed as:

$$s = e + b_0\Pi_t^{-r}e + \vartheta(t) \tag{5}$$

Where ${}_0\Pi_t^{-r}$ is fractional order integral term for eliminating the system steady state error; b are constant values; $\vartheta(t) = \vartheta(0)\exp^{-t/D}$, D is the constant determining the rate of convergence of $\vartheta(t)$.

The derivation of Eq. (5) is obtained:

$$\begin{aligned} \dot{s} &= \dot{e} + b_0\Pi_t^{1-r}e + \dot{\vartheta}(t) \\ &= -\frac{\left(1.5pi_q\varphi_f - T_L - B\omega\right)}{J} + b_0\Pi_t^{1-r}e - \frac{\vartheta(0)}{D}\exp^{-t/D} \end{aligned} \tag{6}$$

To improve the operating quality of the system, the speed controller is designed using the exponential reaching law and the controller expression is given as:

$$\begin{aligned} i_q = \frac{2J}{3p\varphi_f}\Bigg[& b_0\Pi_t^{1-r}e - \frac{\vartheta(0)}{D}\exp^{-t/D} \\ & + \frac{T_L}{J} + \frac{B}{J}\omega + \varepsilon sign(s) + ks\Bigg] \end{aligned} \tag{7}$$

Where ε, k are constant values. From Eq. (7), it can be seen that the i_q contains discontinuous sign function, which can cause a lot of chattering, and affect the control accuracy of the system of the system.

3.2 Design of Reaching Law

To further improve the operation quality of the system, the well-known second-order sliding mode reaching law (SOSMRL), i.e., the super-twisting algorithm [13], is used in this paper instead of the exponential reaching law, which is expressed as follows:

$$\begin{aligned} \dot{x} &= -\beta_1\|^{\frac{1}{2}}sign(x) + \mathrm{y} \\ \dot{y} &= -\beta_2 sign(x) + \dot{\sigma} \end{aligned} \tag{8}$$

When $|\dot{\sigma}| \le \gamma$, then:

$$\begin{cases} \beta_1 > 2 \\ \beta_2 > \dfrac{\beta_1^3 + (4\beta_1 - 8)\gamma^2}{4\beta_1^2 - 8\beta_1} \end{cases} \tag{9}$$

From Eq. (8) and Eq. (9), it can be seen that the SOSMRL suppresses the sliding mode chattering by placing the switching function term containing a large gain into the integral part. However, its proportional part is calculated as an open square, which leads to a slight lack of the system's ability to cope with disturbances [14].

Therefore, this paper designs a NSOSMRL with the basic form:

$$\begin{aligned} \dot{x} &= -\beta_1|x|^{\frac{1}{2}}sigmoid(x) + \lambda x + \mathrm{y} \\ \dot{y} &= -\beta_2 sigmoid(x) + \dot{\sigma} \end{aligned} \tag{10}$$

Where λx is the linear term. From Eq. (10), it can be seen that compared with Eq. (8), there is one more linear term in the proportional part of NSOSMRL, which can enhance the convergence speed of the system by reasonably taking the value of λ and thus improve the system's anti-disturbance ability; secondly, the purpose of further weakening the chattering is reached by adopting the continuous sigmoid function instead of the sign function at the zero point in Eq. (10), and the basic expression of which is:

$$sigmoid(x) = \frac{2}{1 + \exp^{-ax}} - 1 \tag{11}$$

Where $a > 0$. As a proof of the stability of Eq. (10), definition:

$$\begin{cases} F_1 = x \\ F_2 = -\int \beta_2 sigmoid\,(F_1)\,dt + \sigma \end{cases} \tag{12}$$

For the system shown in Eq. (10), the Lyapunov function is chosen as:

$$V(F_1, F_2) = \Im^T\Pi\Im \tag{13}$$

Where $\Im^T = [\Im_1, \Im_2] = \left[\sqrt{|F_1|}sigmoid\,(F_1), F_2\right]$, Π is a real symmetric positive definite matrix, taken as:

$$\Pi = \begin{bmatrix} 4\beta_2 + \left(\beta_1 + \lambda\sqrt{|F_1|}\right)^2 & -\beta_1 - \lambda\sqrt{|F_1|} \\ -\beta_1 - \lambda\sqrt{|F_1|} & 2 \end{bmatrix} \tag{14}$$

The derivative of Eq. (3) can be obtained:

$$\begin{aligned} \dot{V}(F_1, F_2) &= \dot{\Im}^T\Pi\Im + \Im^T\Pi\dot{\Im} \\ &= \frac{1}{2\,|\Im_1|}\left(\Im^T A^T\Pi\Im + \Im^T\Pi A\Im + \rho B^T\Pi\Im + \rho\Im^T\Pi B\right) \end{aligned}$$

$$\leq \frac{1}{2|\Im_1|}\left[\left(\Im^T A^T \Pi\Im + \Im^T \Pi A\Im + \rho B^T \Pi\Im + \rho\Im^T \Pi B\right) + \gamma^2 \Im^2{}_1 - \rho^2\right]$$

$$\leq \frac{1}{2|\Im_1|}\left(\Im^T A^T \Pi\Im + \Im^T \Pi A\Im + \gamma^2 \Im^T C^T C\Im + \Im^T \Pi B B^T \Pi\Im\right)$$

$$= \frac{1}{2|\Im_1|}\left(\Im^T A^T \Pi\Im + \Im^T \Pi A\Im + \Im^T \gamma^2 C^T C\Im + \Im^T \Pi B B^T \Pi\Im\right)$$

$$= -\frac{1}{2|\Im_1|}\Im^T Q\Im \tag{15}$$

Where $A = \begin{bmatrix} -\beta_1 - \lambda\sqrt{|F_1|} & 1 \\ -2\beta_2 & 0 \end{bmatrix}$, $B = \begin{bmatrix} 0 \\ 1 \end{bmatrix}$ $C = \begin{bmatrix} 1 & 0 \end{bmatrix}$, $\rho = 2\sqrt{|F_1|}\dot{\sigma} = 2|\Im_1|\dot{\sigma}$, $\dot{\sigma} \leq \frac{1}{2}\gamma$, $Q = -(A^T\Pi + \Pi A + \gamma^2 C^T C + \Pi B B^T \Pi)$.

For $V(F_1, F_2) \leq 0$, then Q is:

$$Q = -\left[A^T\Pi + \Pi A + \delta^2 C^T C + \Pi B B^T \Pi\right]$$

$$= \begin{bmatrix} 2\left(\beta_1 + \lambda\sqrt{|F_1|}\right)^3 - \left(\beta_1 + \lambda\sqrt{|F_1|}\right)^2 + 4\beta_2\left(\beta_1 + \lambda\sqrt{|F_1|}\right) - \gamma^2 & 2\left(\beta_1 + \lambda\sqrt{|F_1|}\right) - 2\left(\beta_1 + \lambda\sqrt{|F_1|}\right)^2 \\ 2\left(\beta_1 + \lambda\sqrt{|F_1|}\right) - 2\left(\beta_1 + \lambda\sqrt{|F_1|}\right)^2 & 2\left(\beta_1 + \lambda\sqrt{|F_1|}\right) - 4 \end{bmatrix} \tag{16}$$

By the Schur complementary lemma, a sufficient condition for Q to be a positive definite matrix can be introduced:

$$\begin{cases} \beta_1 > 2 \\ \beta_2 > \dfrac{\left(\beta_1 + \lambda|F_1|^{0.5}\right)^2}{4\beta_1 + 4\lambda|F_1|^{0.5} - 8} + \dfrac{\gamma^2}{4\beta_1} \\ \lambda > 0 \end{cases} \tag{17}$$

Combining Eq. (10) and Eq. (6) obtains:

$$i_q = \frac{2J}{3p\varphi_f}\left[b_0\Pi_t^{1-r}e - \frac{\vartheta(0)}{D}\exp^{-t/D} + \frac{TL}{J} + \frac{B}{J}\omega + \beta_1|s|^{\frac{1}{2}}sigmoid(s) + \lambda s + \beta_2 sigmoid(s)\right] \tag{18}$$

4. Stabilization Analysis

To demonstrate the stability of the designed controller, the following Lyapunov function is defined:

$$V_2 = \frac{1}{2}s^2 \tag{19}$$

The derivation of Eq. (18) is obtained:

$$\begin{aligned} \dot{V}_2 &= s \cdot \dot{s} \\ &= s\left[\dot{e} + b_0\Pi_t^{1-r}e + \dot{\vartheta}(t)\right] \\ &= s\left[-\frac{\left(1.5pi_q\varphi_f - T_L - B\omega\right)}{J} + b_0\Pi_t^{1-r}e - \frac{\vartheta(0)}{D}\exp^{-t/D}\right] \\ &= s\left[-\beta_1|s|^{\frac{1}{2}}sigmoid(s) - \lambda s - \beta_2 sigmoid(s)\right] \\ &\leq -\beta_1|s|^{\frac{3}{2}} - \lambda s^2 - \beta_2|s| \end{aligned} \tag{20}$$

From Eq. (19), it can be seen that the value of Eq. (17) can be taken to ensure that $\dot{V}2 \leq 0$, the system is stable.

5. Simulations

In order to verify the validity of the designed, this paper uses MATLAB/Simulink as a platform for simulation research. The parameters of the used PMSM motor are shown in Table 1.

5.1 Load Disturbance Verification

The system is started in no-load mode with a given speed of 1000 Rpm. The simulated waveforms are shown in Fig. 1 for an increase of 20 N·m and a decrease of 20 ·Nm at 0.2 s and 0.4 s, respectively. Additionally, the parameters for each controller are as follows: SMC: $\varepsilon = 200000$, $k = 200$; FOI-SMC: $b = 5$, $r = 0.00000001$, $\varepsilon = 200$, $k = 150$; FOI-SOSMC: $b = 5$, $r = 0.00000001$, $\beta_1 = 1500$, $\beta_2 = 6000$; FOI-NSOSMC: $b = 5$, $r = 0.00000001$, $\lambda = 1000$, $\beta_1 = 500$, $\beta_2 = 6000$.

According to Fig. 1, it can be seen that the SMC has large speed overshoot in the startup phase and load change phase, the longest adjustment time, and the largest speed fluctuation of 0.6 Rpm. Compared with the SMC, the FOISMC with the introduction of fractional-order integral

Table 1 Motor parameters.

Parameters	Value
Sator resistance	2.875 Ω
Magnetic flux	0.175 Wb
Pole number	4
Stator inductance	0.0085 H
Rotational inertia	0.003 kg·m^2
Damping coefficient	0.001 N·m

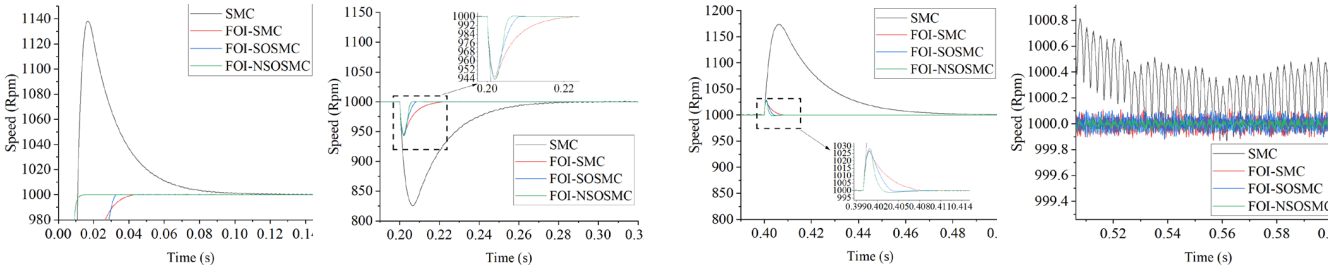

Fig. 1 The speed response under load change.

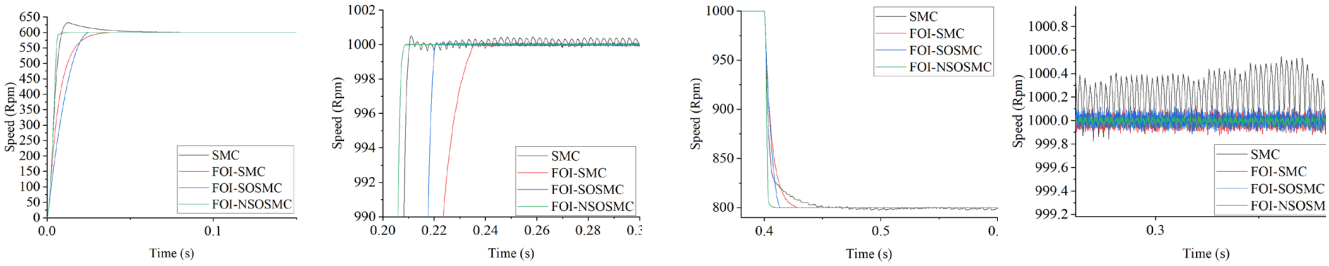

Fig. 2 The speed response under speed change.

sliding-mode surface can effectively suppress sliding-mode chattering, and the speed fluctuation is smaller, 0.2 Rpm, and it can effectively cope with the load disturbance, without startup overshoot. Compared to FOI-SMC, FOI-SOSMC with the introduction of SOSMRL can better cope with load disturbances and its regulation time is smaller. For this reason, the NSOSMRL-based FOI-NSOSMC has the fastest response and the smallest speed fluctuation of 0.1 Rpm by rationally designing the linear term.

5.2 Speed Change Verification

From Fig. 2, compared with the SMC based on linear sliding mode surface, FOI-SMC, FOI-SOMSC and FOI-NSOSMC introducing fractional-order integral sliding mode surface can effectively track the actual speed, among which the FOI-NSOSMC introducing NSOSMRL has the fastest response speed, and it can effectively inhibit the sliding mode chattering with the smallest speed fluctuation, so as to increase the control accuracy of the system.

6. Conclusions

In this paper, a new second-order sliding mode reaching law is proposed by introducing a linear term based on the traditional second-order sliding mode reaching law, which is combined with a fractional-order integral sliding mode surface to design a speed controller for PMSM. And it is compared and analyzed with the traditional SMC, FOI-SMC, and FOI-SOSMC. The simulation results show that the designed FOI-NSOSMC can effectively suppress chattering, and the system dynamic and static characteristics are good, which can effectively improve the system control quality.

Acknowledgments

This work is supported by the Scientific and Technological Research Project in Henan Province (232102241039).

References

[1] D. Fu, X. Zhao, and J. Zhu, "A novel robust super-twisting nonsingular terminal sliding mode controller for permanent magnet linear synchronous motors," IEEE Trans. Power Electron., vol.37, no.3, pp.2936–2945, 2021.

[2] V.I. Utkin and A.S. Poznyak, "Adaptive sliding mode control," Advances in Sliding Mode Control: Concept, Theory and Implementation, vol.1, no.1, pp.21–53, 2013.

[3] X. Yu, Z. Man, and B. Wu, "Design of fuzzy sliding-mode control systems," Fuzzy Sets and Systems, vol.95, no.3, pp.295–306, 1998.

[4] J. Fei and H. Ding, "Adaptive sliding mode control of dynamic system using RBF neural network," Nonlinear Dyn., vol.70, no.1, pp.1563–1573, 2012.

[5] Y. Pan, C. Yang, L. Pan, and H. Yu, "Integral sliding mode control: performance, modification, and improvement," IEEE Trans. Ind. Informat., vol.14, no.7, pp.3087–3096, 2017.

[6] Mu, Zhongcui, et al., "Permanent magnet synchronous motor MPTC system based on FOSM-MRAS observer," Electric Machines & Control, vol.24, no.4, pp.121–130, 2020 (in Chinese).

[7] L. Zhang, R. Tao, Z.-X. Zhang, Y.-R. Chien, and J. Bai, "PMSM non-singular fast terminal sliding mode control with disturbance compensation," Information Sciences, vol.642, no.1, p.119040, 2023.

[8] S. Krim, S. Gdaim, and M.F. Mimouni, "Robust direct torque control with super-twisting sliding mode control for an induction motor drive," Complexity, vol.2019, no.1, pp.1–24, 2019.

[9] F.F.M. El-Sousy and F.A.F. Alenizi, "Optimal adaptive super-twisting sliding-mode control using online actor-critic neural networks for permanent-magnet synchronous motor drives," IEEE Access, vol.9, no.1, pp.82508–82534, 2021.

[10] R. Matušů, "Application of fractional order calculus to control theory," International Journal of Mathematical Models and Methods in Applied Sciences, vol.5, no.7, pp.1162–1169, 2011.

[11] Y.I Son, "Robust performance analysis of a load torque observer for PMSM using singular perturbation theory," IEICE Trans. Fundamentals, vol.E95-A, no.2, pp.604–607, Feb. 2012.

[12] S. Mobayen, A.N. Vargas, L. Acho, G. Pujol-Vázquez, and C.F. Caruntu, "Stabilization of two-dimensional nonlinear systems through barrier-function-based integral sliding-mode control: application to a magnetic levitation system," Nonlinear Dyn., vol.111, no.2, pp.1343–1354, 2023.

[13] J.A. Moreno and M. Osorio, "Strict Lyapunov functions for the super-twisting algorithm," IEEE Trans. Autom. Control, vol.57, no.4, pp.1035–1040, 2012.

[14] L. Zhang, S. Wang, and J. Bai, "Fast-super-twisting sliding mode speed loop control of permanent magnet synchronous motor based on SVM-DTC," IEICE Electron. Express, vol.18, no.1, p.20200375, 2021.